BNL-222833-2022-JAAM

On the Sensitivity to Density-Functional Approximations for CO Binding Energies of Single-Atom Catalysts in Nitrogen-Doped Graphene

Q. Wu

To be published in "ChemPhysChen"

February 2022

Center for Functional Nanomaterials

Brookhaven National Laboratory

U.S. Department of Energy

USDOE Office of Science (SC), Basic Energy Sciences (BES) (SC-22)

DISCLAIMER

On the sensitivity to density-functional approximations for CO binding energies of single-atom catalysts in nitrogen-doped graphene

Dr. Qin Wu*, Dr. Guangjin Wang[1], Dr. Mingjie Liu[2]
Center for Functional Nanomaterials, Brookhaven National Laboratory, Upton, NY 11973
* qinwu@bnl.gov
1. current address: School of Materials Science and Hydrogen Energy, Foshan University, Foshan 528000, P. R. China
2. current address: Department of Chemical Engineering, MIT, Cambridge, MA 02139

Abstract

Density functional theory (DFT) methods are the working horse in screening new catalytic materials. They are widely used to predict trends in binding energies, which are then used to compare the activity of different materials. The binding strength of CO is an important descriptor to the CO_2 reduction catalytic activity of the single transition metal atoms embedded on nitrogen-doped graphene (TM/NG). In this work, however, we show that CO binding strengths in different TM/NG has very different sensitivity to DFT methods. Specifically, Fe/NG CO binding energy changes dramatically with the percentage of exact exchange in the functional; Co/NG does less so, while Ni/NG nearly has no change. Such varying behaviors is a direct result of different local spin configurations, similar to the performance of DFT methods for metal porphyrin complexes. Therefore, caution should be exercised when using DFT binding energies for quantitative predictions in TM/NG single atom catalysis.

Introduction

Electrochemical reduction of CO_2 using renewable energy source is a promising and challenging approach to reducing the CO_2 concentration in atmosphere.[1] It has stimulated a lot of research in finding low-cost and high efficiency electrocatalysts. Nitrogen-doped porous carbon materials with dispersed transition metal (TM) atoms can be prepared inexpensively and often act as excellent single atom catalysts.[2, 3] Therefore, they are actively pursued as a promising alternative for electrochemical CO_2 reduction both theoretically and experimentally.[4-15] Theoretical studies of such porous carbon systems often use nitrogen-doped graphene (NG) as the model support for TM atom embedding.[5, 8, 10, 11, 15] Indeed, when four N atoms are placed around a double vacancy in graphene, a porphyrin-like structure is formed. Porphyrins can chemically bind different metal atoms to form stable complexes. It is thus reasonable to expect atomically dispersed TM in N-doped carbon materials adopts metalloporphyrin-like

structures, which is often supported by X-ray absorption measurements experimentally.[16] With a structure model of the TM/NG catalysts, theoretical studies of its catalytic activity towards CO_2 reduction are often focused on the binding energies of some important intermediates such as *CO. The binding energy of CO is of particular importance because of its implication in the reduction product. Namely, CO will be the main product if the catalyst binds CO weakly and CO readily desorbs from the catalyst. If the catalyst adsorbs CO strongly, CO may be further reduced to make other products such CH_4.

Like many other properties in heterogeneous catalysis, calculation of CO adsorption energy to the catalyst surface is almost exclusively done with semi-local approximation of density functional theory (DFT) methods using a supercell and periodic boundary condition (PBC), even though sometimes the accuracy of such calculations can be questionable.[17] For the TM/NG systems, because of the structural similarity to metalloporphyrin, it is possible to discuss its electronic property in the context of metal complex and quantum chemistry. When a single transition metal atom is stabilized by the porphyrin-like structure on N-doped graphene, its local electronic state could have spin polarization, similar to be in a spin state other than singlet for metal complexes. In PBC, it means the unit cell that contains the TM/NG moiety has a magnetization corresponding to the number of unpaired electrons, which most likely reside on the metal center. Furthermore, the transition metal center enables facile spin crossover. Therefore, its local spin state can change in order to stay on the lowest energy path when reactions occur, such as CO binding. For instance, iron porphyrins are well studied because of its relevance to heme. It has been shown that the triplet Fe-porphyrin becomes a singlet upon an additional axial ligand such as CO.[18] To get the correct energy change computationally, it is important to use a method that works equally well for both high-spin and low-spin states.[19] This is unfortunately not true for many DFT methods.[20, 21] Results are often very sensitive to the mixing of exact exchange used in the approximation.[22, 23] If local spin states in TM/NG have similar complexity to that in metalloporphyrin, sensitivity of their calculated CO adsorption energies to DFT methods should be examined.

In this work, we investigate the DFT results of CO binding energies for three different TM/NG systems (TM=Fe, Co, Ni). We use both plane waves and local basis of gaussians with periodic

boundary conditions and confirm different bases give the same results. Using local basis to compare hybrid and non-hybrid functionals, we find that the three systems have very different sensitivity to exact exchange (EXX). We further highlight this difference by using molecular analog systems for which the amount of EXX can be tuned. For the strong sensitivity in Fe/NG, we also discuss its origin and the feasibility of a potential remedy.

Computational Methods

Computations are carried out with both the plane-wave code VASP 5.4.4[24, 25] and local-basis code Gaussian 16.[26] With VASP, the TM/NG system is modeled by a rectangular fixed graphene supercell (12.34 Å x12.82 Å) with 16 Å vacuum region in the perpendicular direction. Two adjacent C atoms are removed to create a double vacancy (DV). The TM atom is placed in the center of DV and different number of N atoms are used to substitute C around the DV (Figure 1). The Bayesian Error Estimation Functionals with added van der Waals corrections (BEEF-vdW)[27] is used to describe the exchange-correlation effect. A plane-wave cutoff energy of 400 eV is used together with PAW-PBE potentials where semi core *p* states are treated as valence.[28] The convergence force in structural relaxation is 0.01 eV/Å. The K point mesh is Monkhorst-Pack 4 × 4 × 1. Gaussian smearing with a width of 0.05 eV is used. All calculations allow spin polarization with no spin-orbit coupling.

Gaussian calculations have been done both with and without the periodic boundary condition (PBC). With PBC, an infinite 2D graphene sheet is simulated without repeat in the perpendicular direction, which is possible because of local basis functions. A 6x6 supercell of primitive graphene lattices is used (Figure 3a), and the same procedures for DV creating, N doping and TM embedding as for VASP calculations. All atoms, as well as both translation vectors (TVs), are allowed to relax. The 2D sheet is studied with both PBE[29] and HSE[30, 31] functionals. A molecular analogue (Figure 3b) of the infinite system is built and verified to give similar results. This molecular analogue is then used to study the dependence on the percentage of exact exchange. All calculations are done with the 6-31G(d) basis set for C, N, O and H, and the LANL2DZ basis set and effective core potential for TM atoms. A larger basis set of 6-311G(d) for all atoms is also used in limited calculations to show that basis set size has little impact on our results. (S4 in SI) The varying percentage of exact exchange is set by following the

instruction from Gaussian manual on "User-Defined Hybrid Models" with the PBE exchange and PBE correlation as components. For example, the popular PBE0 hybrid functional, which has 25% of exact exchange, can be specified by the following route section in the input file.

#P PBEPBE IOp(3/76=1000002500) IOp(3/77=0750007500) IOp(3/78=1000010000)

Results

From BEEF-vdW, PBC and plane waves in VASP

Figure 1 displays the structure of TM embedded in a DV graphene with different level of N doping, all the way up to 4 N atoms, around the DV. It has a porphyrin-like structure, which together with the TM atom in the center has alternating 5- or 6-membered rings. Due to symmetry, there is only one unique structure for 1, 3 and 4 N atoms. 2 N's can have three different arrangements. The one with both N atoms in the same 6-membered ring has the lowest energy (N2 in Figure 1) and will be our choice in subsequent calculations.

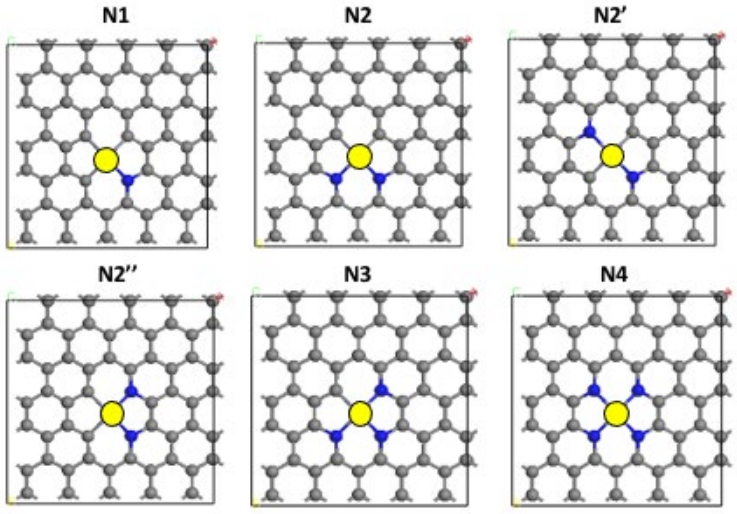

Figure 1. Embedded metal atom (yellow) with different nitrogen (blue) doping levels.

We next examine the electronic properties of TM/NG in N0, N1, N2, N3 and N4 configurations. N0 means no N atom around the DV, while others are shown in Figure 1. We choose to focus on the total magnetization, which, in the unit of Bohr magneton, is equal to the difference between the numbers of spin-up and spin-down electron in the unit cell. For a molecule this difference corresponds to unpaired electrons and defines its spin multiplicity. While we cannot consider the spin multiplicity of a unit cell in a periodic system, we can compare their local electronic configurations based on the number of unpaired electrons. Using the tag LORBIT=11, we have

checked that the magnetization, i.e. unpaired electrons, concentrates on the *d* orbitals of the metal center as expected. This supports our focus on the magnetization of a unit cell and compare it to spin states of metal complexes in the following discussion. For all our calculations, we have used the tag MAGMOM to start from initial configurations with a large number (i.e. 5) of unpaired electrons on the metal center. Because graphene is a semi-metal with continuous density of states at the Fermi level, and we use a finite K-point sampling and Gaussian smearing, orbitals around the Fermi level are partially occupied.[32] Therefore, the number of unpaired electrons can be a non-integer. This is evident from the results shown in Figure 2. Due to partial occupancies of orbitals, the unpaired electrons can be nearly zero even when the total number of electrons in a unit cell is an odd number, such as in Ni/N3G. Our results for TM/N0G agree with a previous study[33], where explanations of the trend is provided. We choose not to present a detailed electronic-structure study of all N-doping configurations. Instead, we note that as the number of N atoms increases, the number of unpaired electrons in Fe, Co and Ni converges to 2, 1 and 0, respectively, as they are expected in a porphyrin-like molecule. This justifies our choice to focus on the N4 structures in the following discussion of spin configurations.

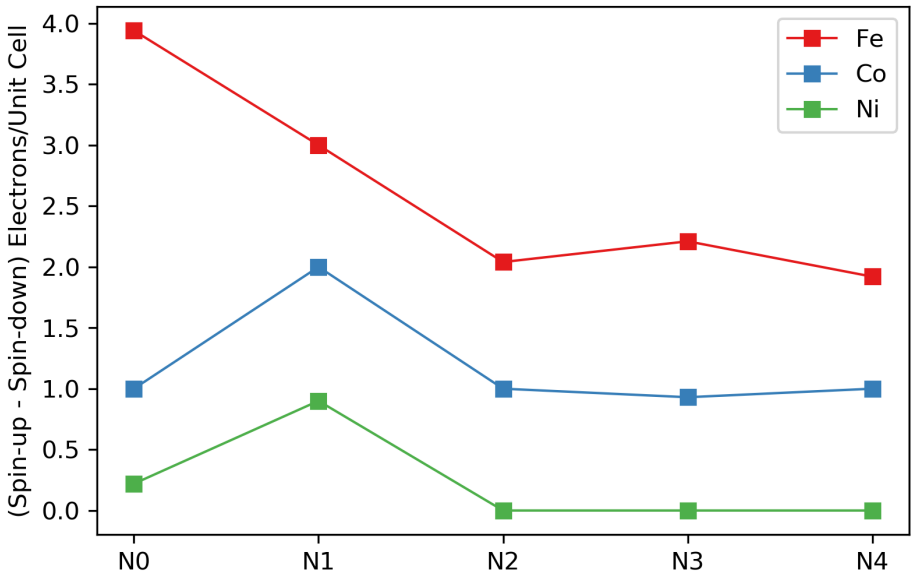

Figure 2. Number of spin-up minus spin-down electrons in a unit cell of different TM/NG using structural models in Figure 1. N0 means no N atom.

We now turn our attention to CO binding. We will only use the N4 structures, i.e. the porphyrin-like one. It is the most used model for single atom catalyst in N-doped graphene. Its similarity to

porphyrin enables easy construction of a molecular analog, which we will use later. At the same time, it also highlights the differences among Fe, Co and Ni. Columns 2 and 3 in Table 1 list the number of unpaired electrons in the unit cell before and after CO adsorption. Fe/N4G goes from having 2 unpaired electrons to no spin polarization after binding CO. This is very similar to the high spin to low spin change in iron-porphyrin complexes.[34] On the other hand, there is no spin configuration change in Ni/N4G after CO binding. Co/N4G has a small change. Also listed in Table 1 is the CO binding energy calculated by E(CO-TM/N4G) – E(CO) – E(TM/N4G). These are the numbers that are used in CO_2 reduction catalyst screening. They suggest that Fe/N4G would not have CO as the main product because its large binding energy at -1.51 eV; and Ni/N4G would mainly produce CO because of its weak CO binding at -0.09 eV. While these results qualitatively agree with experimental observations,[4, 35, 36] the magnitude of their difference is surprising. With the understanding that these binding energies are calculated from different spin configuration changes, we will further probe reliability of these numbers. we want to compare the results with those from a hybrid functional, i.e. with added exact exchange (EXX). Although the screened hybrid functional HSE is available in VASP, it is not efficient enough for our purpose. On the other hand, we find HSE calculations of 2D periodic systems are quite efficient in Gaussian 16. In the following subsection, we present our results from Gaussian 16.

Table 1. Number of unpaired electrons in the unit-cell of TM/N4G before and after CO adsorption. Also listed is the CO binding energy.

TM	TM/N4G	CO-TM/N4G	Binding Energy (eV)
Fe	1.9	0.0	-1.51
Co	1.0	0.5	-0.53
Ni	0.0	0.0	-0.09

From PBC and local basis functions in Gaussian 16

Because it uses local basis functions, Gaussian 16 can limit its periodicity to lower dimensions. This feature is convenient for 2D materials like graphene, which also explains its efficiency for hybrid functionals like HSE. The available PBC options in Gaussian 16, however, do not have occupancy smearing around the Fermi level. Instead, the number of unpaired electrons in a unit cell is fixed by the spin multiplicity specified in the input file. It should be noted that spin multiplicity is not meaningful for unit cells of an extended system. Therefore, the terms

"singlet", "doublet" and "triplet" used here should be understood as indication of 0, 1, and 2 unpaired electrons in the unit cell, respectively. In Table 2 and 3 we have summarized the results for PBE and HSE, respectively. For TM/N4G and CO-TM/N4G, the tables list their spin states with the lowest energies, which are subsequently used to calculate the CO binding energies. The PBE binding energies in Table 2 agree well with BEEF-vdW results in Table 1. There is only 0.02 eV difference for Fe/N4G and Ni/N4G. The slightly greater difference for Co/N4G is possibly due to the difference in the spin configuration of CO-Co/N4G. The fractional magnetization of 0.5 from VASP in not accessible to Gaussian. It is reassuring to see that results from VASP and Gaussian are almost identical when the same spin states are reached as in Fe/N4G and Ni/N4G.

Table 2. PBC Gaussian 16 results of the PBE functional. The relaxed translation vectors for all systems are nearly identical with lengths of 14.77 (±0.01) Å and 14.93 (±0.01) Å and form a 59.6º angle. (See S2 in SI for details) The lowest energy spin state is specified for all TM/N4G before and after CO adsorption. The binding energy is taken as E(CO-TM/N4G) – E(CO) – E(TM/N4G). The energy differences between singlet and triplet for Fe/N4G and Ni/N4G are also reported.

TM	TM/N4G	CO-TM/N4G	Binding Energy (eV)	E_S - E_T of TM/N4G (eV)
Fe	"triplet"	"singlet"	-1.53	0.91
Co	"doublet"	"doublet"	-0.70	n/a
Ni	"singlet"	"singlet"	-0.11	-0.78

Table 3. PBC Gaussian 16 results of the HSE functional. The relaxed translation vectors for all systems are nearly identical with lengths of 14.67 (±0.01) Å and 14.83 (±0.01) Å and form a 59.6º angle. The lowest energy spin state is specified for all TM/N4G before and after CO adsorption. The binding energy is taken as E(CO-TM/N4G) – E(CO) – E(TM/N4G). The energy differences between singlet and triplet for Fe/N4G and Ni/N4G are also reported.

TM	TM/N4G	CO-TM/N4G	Binding Energy (eV)	E_S - E_T of TM/N4G (eV)
Fe	"triplet"	"singlet"	-0.45	1.69
Co	"doublet"	"doublet"	-0.39	n/a
Ni	"singlet"	"singlet"	-0.08	-0.88

Comparing Table 2 and 3, we note that PBE and HSE give the same lowest-energy spin configurations for all TM/N4G and CO-TM/N4G systems. However, the CO binding energy of Fe/N4G is 1.1 eV stronger from PBE than from HSE! Such a big difference casts serious doubt on the choice of DFT methods. For Co/N4G, the same comparison gives 0.3 eV, a more modest but still significant difference. On the other hand, the CO binding energy of Ni/N4G changes only by 0.03 eV from PBE to HSE. The size of this energy shift follows the same trend as the

number of unpaired electrons in Fe/N4G, Co/N4G and Ni/N4G, which suggests that different spin configuration within each TM/NG system might already pose great difficulty to DFT methods. To verify this idea, we also list the energy difference between "singlet" and "triplet" for Fe/N4G and Ni/N4G in Tables 2 and 3. Indeed, the "singlet"-"triplet" energy difference for Fe/N4G is 0.8 eV between HSE and PBE, while the same quantity for Ni/N4G is only 0.1 eV.

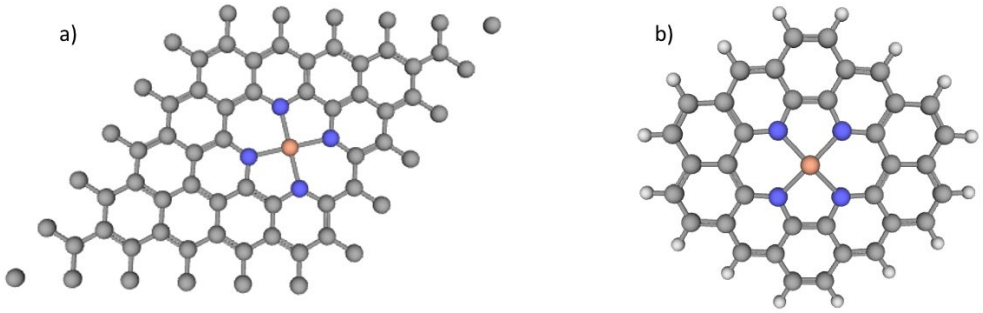

Figure 3. Unit cell (a) and the molecular analog (b) of Fe/NG in Gaussian16 calculations.

Exact exchange dependence

A commonly used tactic in developing more accurate DFT approximations is to tune the amount of exact exchange in the functional to match benchmark results. To test whether this approach can work for TM/NG systems, we decide to use user-defined hybrid models as specified in **Computational Methods**. Such capability is only available for global hybrid functionals, whose long-range exact exchange is unfeasible for PBC calculations. We resort to a molecular analog of TM/NG (Figure 3b), which is a carved-out graphene flake with all dangling bonds capped with hydrogen atoms. We label the molecular analog TM/P and find the PBE CO binding energy for Fe/P, Co/P and Ni/P is -1.73, -0.74 and -0.11 eV, respectively. These numbers are in reasonable agreement with those in Table 2, supporting the use of these analogs for studying trends in TM/NG systems.

We now probe the trends in CO binding energy and singlet-triplet energy difference when the percentage of EXX is increased from 0 to 90%. For these calculations, we have fixed the geometry of each system to its PBE optimized value. Therefore, when EXX percentage changes, only single-point calculations are done. The singlet-triplet energy difference is an adiabatic gap. The CO binding energy for Fe/P is calculated using the triplet state of Fe/P and singlet of CO-Fe/P. For Co/P, it is both doublets before and after CO binding; for Ni/P, both singlets. Figure 4

shows the results. It is interesting to see that the CO binding energy almost increases linearly with the EXX%. More importantly, the slope for each system is very different with Fe/P > Co/P > Ni/P. The dramatic differences between PBE and HSE in earlier PBC calculations follow these trends, considering that HSE has 25% of short-range EXX. While PBE and HSE agree on the order of CO binding energy for Fe/NG, Co/NG and Ni/NG, Figure 4 shows that even the order can change if a functional with more EXX is used. It is thus important to benchmark DFT methods against more accurate methods for these systems.

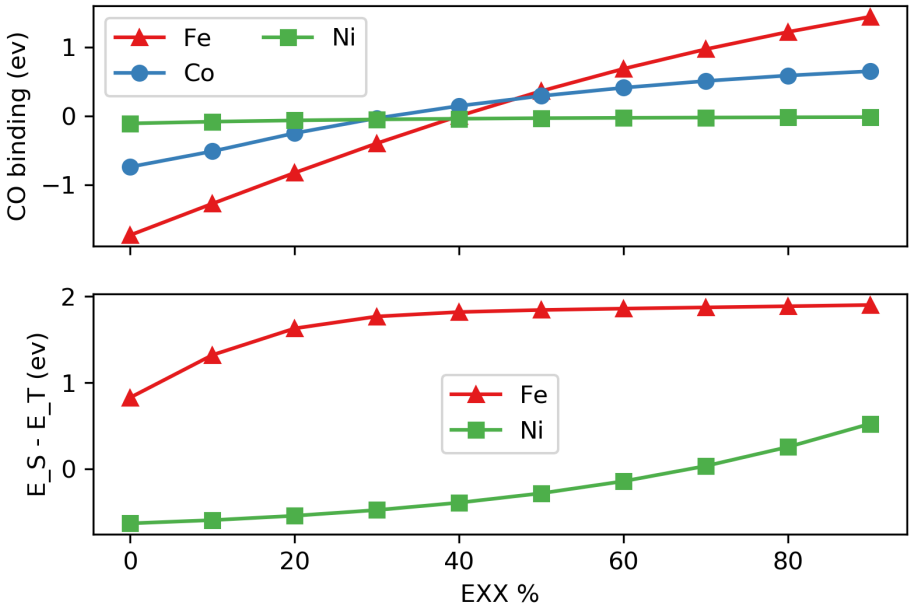

Figure 4. Dependence of CO binding energy (top) and singlet-triplet adiabatic energy difference (bottom) on the percentage of exact exchange in the user defined functionals.

Highly accurate correlated wave function methods are often used to benchmark DFT methods, and they become increasingly available for periodic systems.[37] Currently, their computational cost is still too high to be applied to TM/NG. Benchmark of Fe-porphyrin with the DLPNO-CCSD(T) method was reported,[38] in which the spin stability trend was found to be reproduced with the hybrid functional B3LYP. However, it also found that multireference characters would make the DLPNO-CCSD(T) results non-definitive, which calls for more expensive methodology. Accurate benchmark of CO binding energies is beyond the capability of our current work. However, we want to test the idea of using singlet-triplet gap (Δ_{ST}) for benchmark instead of CO

binding energy. Specifically, we want to see if Δ_{ST} has the same dependence on EXX% as CO binding energy. Because Δ_{ST} does not apply to Co/P, Figure 4 only shows the results for Fe/P and Ni/P. Interestingly, Δ_{ST} follows the trend of CO binding energy pretty well for EXX% range of 0 to 30%. After that, Δ_{ST} for Fe/P becomes much flatter than CO binding, while the opposite happens for Ni/P. Therefore, it is possible to use Δ_{ST} to benchmark DFT methods for CO binding energy, provided that the percentage of EXX is controlled under 30%. One caveat in our argument is that iron-porphyrin is known to have a lower energy open-shell singlet state than the closed-shell singlet in DFT calculations.[20, 39, 40] We, however, have used the closed-shell singlet of Fe/P in the comparison, which is similar to the singlet state of CO-bound Fe/P and thus more appropriate here.

Conclusion

Single transition metal atoms embedded on nitrogen-doped graphene (TM/NG), for its similarity to metal porphyrin complexes, can be viewed as a bridge between heterogenous and molecular catalysts. In this work, by focusing on the CO binding energy, a key indicator in catalytic CO_2 reduction, we have shown that DFT calculations with either plane waves or local basis give the same results. Taking a molecular approach from the perspective of local spin configurations, we are able to show that CO binding energy in different TM/NG has very different sensitivity to DFT methods. Specifically, the CO binding strength of Fe/NG changes dramatically with the EXX percentage in the functional. It is less so for Co/NG, while Ni/NG nearly has no change. Such varying behaviors are related to their different local spin configurations, as well as the presence of spin crossover in Fe/NG, similar to the performance of DFT methods for metal porphyrin complexes. For the most common range of EXX percentage, the singlet-triplet energy gap in iron porphyrin presents the same sensitivity as its CO binding energy, suggesting the DFT approximate functional could be tuned against accurate correlated wavefunction methods by comparing the singlet-triplet energy gap. Without such benchmarks, great care should be taken when using DFT binding energies for quantitative predictions in TM/NG single atom catalysis.

Key Words

CO_2 reduction, density functional approximation, nitrogen-doped graphene, porphyrin-like singlet atom catalysts, spin configurations

Acknowledgement

This research is carried out at the Center for Functional Nanomaterials, which is a U.S. DOE Office of Science Facility, and used resource at the Scientific Data and Computing Center of the Computational Science Initiative, at Brookhaven National Laboratory under Contract No. DE-SC0012704. G.W. thanks the financial support by the National Natural Science Foundation of China (No. 21802037).

References:

[1] S. Jin, Z. Hao, K. Zhang, Z. Yan, J. Chen, *Angew Chem Int Ed* **2021**, 60, 20627-20648.
[2] A.S. Varela, W. Ju, A. Bagger, P. Franco, J. Rossmeisl, P. Strasser, *ACS Catalysis* **2019**, 9, 7270-7284.
[3] T. Möller, W. Ju, A. Bagger, X. Wang, F. Luo, T. Ngo Thanh, A.S. Varela, J. Rossmeisl, P. Strasser, *Energy & Environmental Science* **2019**, 12, 640-647.
[4] X.-M. Hu, H.H. Hval, E.T. Bjerglund, K.J. Dalgaard, M.R. Madsen, M.-M. Pohl, E. Welter, P. Lamagni, K.B. Buhl, M. Bremholm, M. Beller, S.U. Pedersen, T. Skrydstrup, K. Daasbjerg, *ACS Catalysis* **2018**, 8, 6255-6264.
[5] K. Jiang, S. Siahrostami, T. Zheng, Y. Hu, S. Hwang, E. Stavitski, Y. Peng, J. Dynes, M. Gangisetty, D. Su, K. Attenkofer, H. Wang, *Energy & Environmental Science* **2018**, 11, 893-903.
[6] W. Ju, A. Bagger, G.P. Hao, A.S. Varela, I. Sinev, V. Bon, B. Roldan Cuenya, S. Kaskel, J. Rossmeisl, P. Strasser, *Nat Commun* **2017**, 8, 944.
[7] X. Li, W. Bi, M. Chen, Y. Sun, H. Ju, W. Yan, J. Zhu, X. Wu, W. Chu, C. Wu, Y. Xie, *J Am Chem Soc* **2017**, 139, 14889-14892.
[8] F. Pan, H. Zhang, K. Liu, D. Cullen, K. More, M. Wang, Z. Feng, G. Wang, G. Wu, Y. Li, *ACS Catalysis* **2018**, 8, 3116-3122.
[9] Y. Pan, R. Lin, Y. Chen, S. Liu, W. Zhu, X. Cao, W. Chen, K. Wu, W.C. Cheong, Y. Wang, L. Zheng, J. Luo, Y. Lin, Y. Liu, C. Liu, J. Li, Q. Lu, X. Chen, D. Wang, Q. Peng, C. Chen, Y. Li, *J Am Chem Soc* **2018**, 140, 4218-4221.
[10] X. Qin, S. Zhu, F. Xiao, L. Zhang, M. Shao, *ACS Energy Letters* **2019**, 4, 1778-1783.
[11] V. Tripkovic, M. Vanin, M. Karamad, M.E. Björketun, K.W. Jacobsen, K.S. Thygesen, J. Rossmeisl, *The Journal of Physical Chemistry C* **2013**, 117, 9187-9195.
[12] A.S. Varela, N. Ranjbar Sahraie, J. Steinberg, W. Ju, H.S. Oh, P. Strasser, *Angew Chem Int Ed* **2015**, 54, 10758-10762.
[13] C. Yan, H. Li, Y. Ye, H. Wu, F. Cai, R. Si, J. Xiao, S. Miao, S. Xie, F. Yang, Y. Li, G. Wang, X. Bao, *Energy & Environmental Science* **2018**, 11, 1204-1210.
[14] H.B. Yang, S.-F. Hung, S. Liu, K. Yuan, S. Miao, L. Zhang, X. Huang, H.-Y. Wang, W. Cai, R. Chen, J. Gao, X. Yang, W. Chen, Y. Huang, H.M. Chen, C.M. Li, T. Zhang, B. Liu, *Nature Energy* **2018**, 3, 140-147.
[15] Z. Zhang, J. Xiao, X.J. Chen, S. Yu, L. Yu, R. Si, Y. Wang, S. Wang, X. Meng, Y. Wang, Z.Q. Tian, D. Deng, *Angew Chem Int Ed* **2018**, 57, 16339-16342.

[16] L. Han, S. Song, M. Liu, S. Yao, Z. Liang, H. Cheng, Z. Ren, W. Liu, R. Lin, G. Qi, X. Liu, Q. Wu, J. Luo, H.L. Xin, *J Am Chem Soc* **2020**, 142, 12563-12567.
[17] L. Schimka, J. Harl, A. Stroppa, A. Gruneis, M. Marsman, F. Mittendorfer, G. Kresse, *Nat Mater* **2010**, 9, 741-744.
[18] M.-S. Liao, S. Scheiner, *J. Chem. Phys.* **2002**, 117, 205-219.
[19] M. Radoń, Chapter Seven - Toward accurate spin-state energetics of transition metal complexes, in: R. van Eldik, R. Puchta (Eds.), *Advances in Inorganic Chemistry*, Academic Press **2019**, pp. 221-264.
[20] M. Radoń, K. Pierloot, *The Journal of Physical Chemistry A* **2008**, 112, 11824-11832.
[21] S. Vancoillie, H. Zhao, M. Radoń, K. Pierloot, *J Chem Theory Comput* **2010**, 6, 576-582.
[22] V.E. Berryman, R.J. Boyd, E.R. Johnson, *J Chem Theory Comput* **2015**, 11, 3022-3028.
[23] T.Z.H. Gani, H.J. Kulik, *J Chem Theory Comput* **2017**, 13, 5443-5457.
[24] G. Kresse, J. Furthmuller, *Comp Mater Sci* **1996**, 6, 15-50.
[25] G. Kresse, J. Furthmuller, *Phys Rev B* **1996**, 54, 11169-11186.
[26] M.J. Frisch, G.W. Trucks, H.B. Schlegel, G.E. Scuseria, M.A. Robb, J.R. Cheeseman, G. Scalmani, V. Barone, G.A. Petersson, H. Nakatsuji, X. Li, M. Caricato, A.V. Marenich, J. Bloino, B.G. Janesko, R. Gomperts, B. Mennucci, H.P. Hratchian, J.V. Ortiz, A.F. Izmaylov, J.L. Sonnenberg, Williams, F. Ding, F. Lipparini, F. Egidi, J. Goings, B. Peng, A. Petrone, T. Henderson, D. Ranasinghe, V.G. Zakrzewski, J. Gao, N. Rega, G. Zheng, W. Liang, M. Hada, M. Ehara, K. Toyota, R. Fukuda, J. Hasegawa, M. Ishida, T. Nakajima, Y. Honda, O. Kitao, H. Nakai, T. Vreven, K. Throssell, J.A. Montgomery Jr., J.E. Peralta, F. Ogliaro, M.J. Bearpark, J.J. Heyd, E.N. Brothers, K.N. Kudin, V.N. Staroverov, T.A. Keith, R. Kobayashi, J. Normand, K. Raghavachari, A.P. Rendell, J.C. Burant, S.S. Iyengar, J. Tomasi, M. Cossi, J.M. Millam, M. Klene, C. Adamo, R. Cammi, J.W. Ochterski, R.L. Martin, K. Morokuma, O. Farkas, J.B. Foresman, D.J. Fox, Gaussian 16 Rev. A.03, Wallingford, CT, **2016**.
[27] J. Wellendorff, K.T. Lundgaard, A. Mogelhoj, V. Petzold, D.D. Landis, J.K. Norskov, T. Bligaard, K.W. Jacobsen, *Phys Rev B* **2012** 85, 235149.
[28] G. Kresse, D. Joubert, *Phys Rev B* **1999**, 59, 1758-1775.
[29] J.P. Perdew, K. Burke, M. Ernzerhof, *Phys Rev Lett* **1996**, 77, 3865.
[30] J. Heyd, G.E. Scuseria, *J. Chem. Phys.* **2004**, 121, 1187-1192.
[31] J. Heyd, G.E. Scuseria, M. Ernzerhof, *J. Chem. Phys.* **2006**,124, 219906.
[32] K.T. Chan, J.B. Neaton, M.L. Cohen, *Phys Rev B* **2008**, 77, 235430.
[33] A.V. Krasheninnikov, P.O. Lehtinen, A.S. Foster, P. Pyykko, R.M. Nieminen, *Phys Rev Lett* **2009**, 102, 126807.
[34] C. Rovira, K. Kunc, J. Hutter, P. Ballone, M. Parrinello, *The Journal of Physical Chemistry A* **1997**, 101, 8914-8925.
[35] C. Zhang, S. Yang, J. Wu, M. Liu, S. Yazdi, M. Ren, J. Sha, J. Zhong, K. Nie, A.S. Jalilov, Z. Li, H. Li, B.I. Yakobson, Q. Wu, E. Ringe, H. Xu, P.M. Ajayan, J.M. Tour, *Advanced Energy Materials* **2018,** 8, 1703487.
[36] P. Yao, J. Zhang, Y. Qiu, Q. Zheng, H. Zhang, J. Yan, X. Li, *ACS Sustainable Chemistry & Engineering* **2021**,9, 5437-5444.
[37] J. McClain, Q. Sun, G.K.-L. Chan, T.C. Berkelbach, *J Chem Theory Comput* **2017**, 13, 1209-1218.
[38] M. Torrent-Sucarrat, I. Arrastia, A. Arrieta, F.P. Cossío, *ACS Catalysis* **2018**, 8, 11140-11153.

[39] M.R.A. Blomberg, A.J. Johansson, P.E.M. Siegbahn, *Inorg Chem* **2007**, 46, 7992-7997.
[40] M. Radoń, *J Chem Theory Comput* **2014**, 10, 2306-2321.